Correcting model biases of CO in East Asia: impact on oxidant distributions during KORUS-AQ

Benjamin Gaubert[1], Louisa K. Emmons[1], Kevin Raeder[2], Simone Tilmes[1], K. Miyazaki[3], Avelino. F. Arellano Jr[4], Nellie Elguindi[5], Claire Granier[5,6], Wenfu Tang[7], Jérôme Barré[8], Helen M. Worden[1], Rebecca R. Buchholz[1], David P. Edwards[1], Philipp Franke[9], Jeffrey L. Anderson[2], Marielle Saunois[10], Jason Schroeder[11], Jung-Hun Woo[12]. Isobel J. Simpson[13], Donald R. Blake[13], Simone Meinardi[13], Paul O. Wennberg[14], John Crounse[14], Alex Teng[14], Michelle Kim[14], Russell R. Dickerson[15,16], Hao He[15,16], Xinrong Ren[15,17]

[1]Atmospheric Chemistry Observations and Modeling, National Center for Atmospheric Research, Boulder, CO, USA.
[2]Computational and Information Systems Laboratory, National Center for Atmospheric Research, Boulder, CO, USA.
[3]Jet Propulsion Laboratory, California Institute of Technology, Pasadena, CA, USA.
[4]Dept. of Hydrology and Atmospheric Sciences, University of Arizona, Tucson, AZ, USA.
[5]Laboratoire d'Aérologie, CNRS, Université de Toulouse, France.
[6]NOAA Chemical Sciences Laboratory-CIRES/University of Colorado, Boulder, CO, USA.
[7]Advanced Study Program, National Center for Atmospheric Research, Boulder, CO, USA.
[8]European Centre for Medium-Range Weather Forecasts, Shinfield Park, Reading, RG2 9AX, UK.
[9]Forschungszentrum Jülich GmbH, Institut für Energie und Klimaforschung IEK-8, 52425 Jülich, Germany.
[10]Laboratoire des Sciences du Climat et de l'Environnement, LSCE-IPSL (CEA-CNRS-UVSQ), Université Paris-Saclay, 91191 Gif-sur-Yvette, France.
[11]California Air Resources Board, Sacramento, CA, USA.
[12]Department of Advanced Technology Fusion, Konkuk University, Seoul, South Korea.
[13]Department Chemistry, University of California, Irvine, Irvine, CA 92697, USA.
[14]California Institute of Technology, Pasadena, CA, USA.
[15]Department of Atmospheric and Oceanic Science, University of Maryland, College Park, MD, USA
[16]Earth System Science Interdisciplinary Center, University of Maryland, College Park, MD, USA
[17]Air Resources Laboratory, National Oceanic and Atmospheric Administration, College Park, MD, USA

Correspondence to: Benjamin Gaubert (gaubert@ucar.edu)

1.Prescribed and emitted Methane

Fig S1 shows how the differences of using prescribed CH_4 and using emissions on the surface level mixing ratios. The prescribed field varies over latitudes and have a maximum of around 1925 ppbv over Korea and Japan. The field with emissions suggests much stronger longitudinal gradients with values larger than 2000 ppbv, between 2000 and 2300 ppbv in Eastern China, 2000 ppbv over south Korea, and less than 1900 ppbv over the ocean. Therefore, the gradients are much larger.

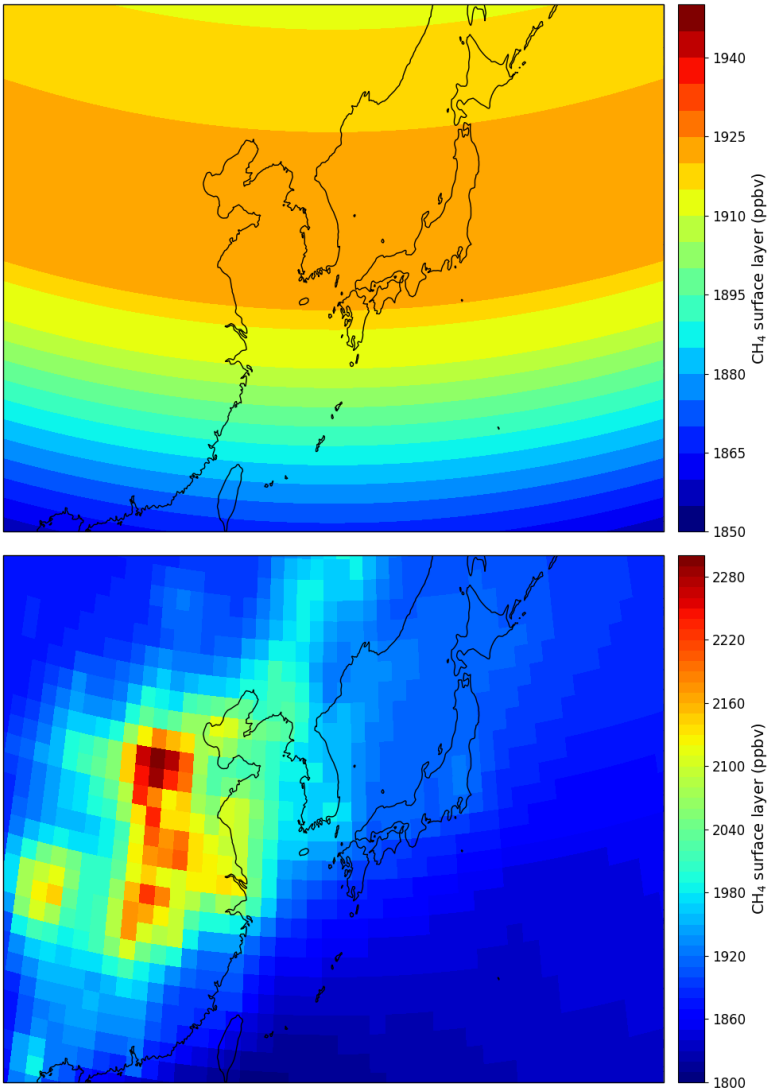

Figure S1: Monthly average (May 2016) CH_4 concentration at the model surface layer. The upper panel shows the standard CAM-Chem that is replace every time step to the CMIP6 lower boundary condition file (CAM-Chem-H2O). The lower panel shows the result using GCP-CH4 emissions (GCP-H2O). Both simulations have the same chemistry and the same setup. Note the different scale.

2. Complementary evaluation of the Control-Run and MOPITT-DA

In this section, we further evaluate the Control-Run and the MOPITT-DA with additional chemicals and physical parameters. Figure S2 show that NO and NO_2 were pretty well simulated on average for the lower levels. The NO_2 photolysis is underestimated, and this is probable explanation of the HNO_3 overestimation. However, the $J(O^1D)$ is only slightly underestimated on average. As in our previous study (Gaubert et al., 2016), the CO assimilation leads to a large increase in H_2O_2, which aggravates the overestimation. Fig. S3, S4, S5 show the comparison of the vertical profiles for H_2O, temperature and wind speed for the different phases and for all the campaign. It overall shows a good agreement with no particular biases for temperature and H_2O. The wind speed is overestimated, except for the phase 4 for which the wind speed in underestimated.

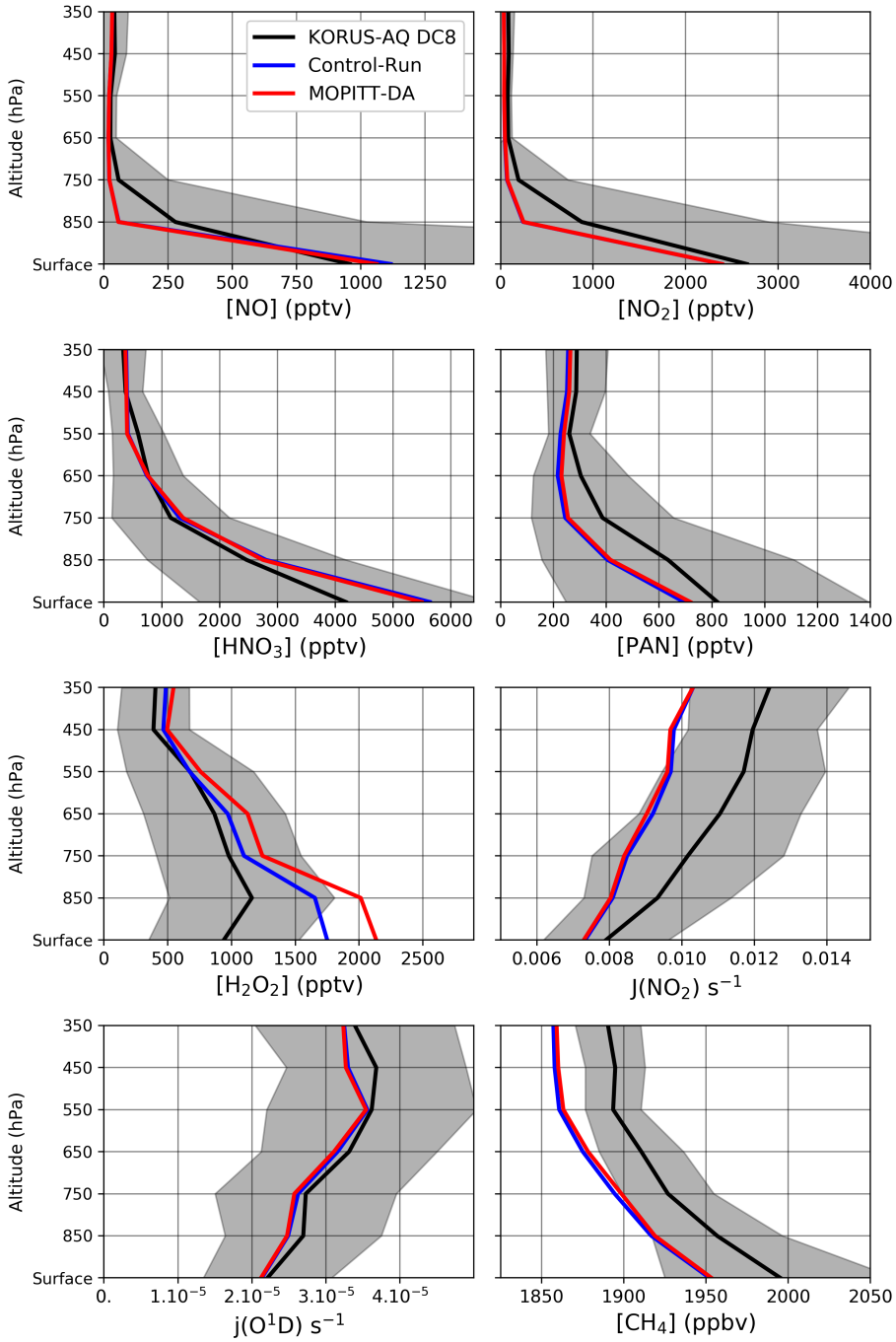

Figure S2: Comparison of DC8 observations of a range of chemical compounds and actinic fluxes during KORUS-AQ. The data are filtered if the Benzene measured by the PTRMS is higher 1 ppbv. Otherwise all the available data, different for each instrument, are used in this plot. Instruments are described in the main manuscript.

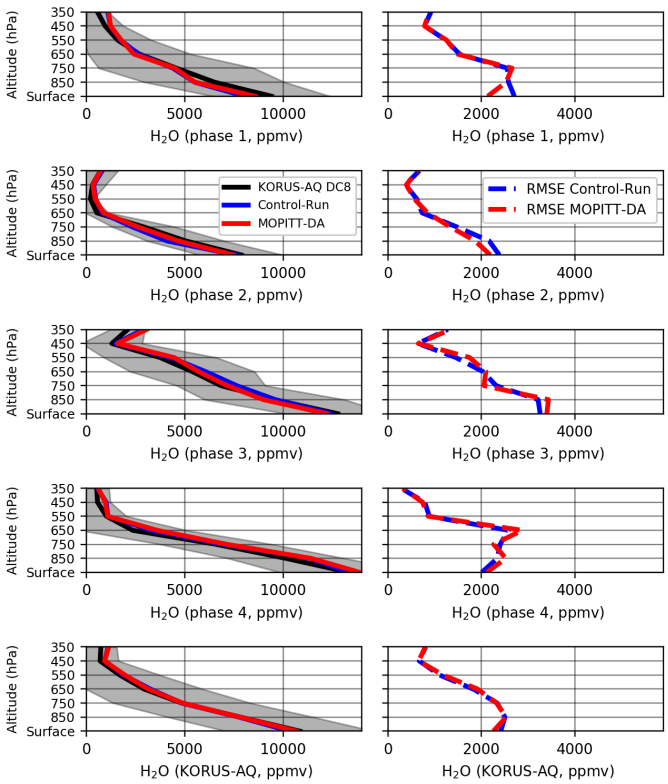

Figure S3: Average water vapor profiles (left panels) and related RMSE (right panels) for the Control-Run and the MOPITT-DA. The mean (black line) and standard deviation (shaded grey) of the observations are calculated for each 100 hPa bins. The first 4 rows are average over the different weather regimes of the campaign (Peterson et al. 2019). The last row is the average over the whole campaign. The only rejected observations are when Benzene measured by the Proton Transfer Reaction – Mass Spectrometry (PTRMS) is higher than 1 ppb, measured only over the highly industrialized Daesan petrochemical complex (Simpson et al., 2020).

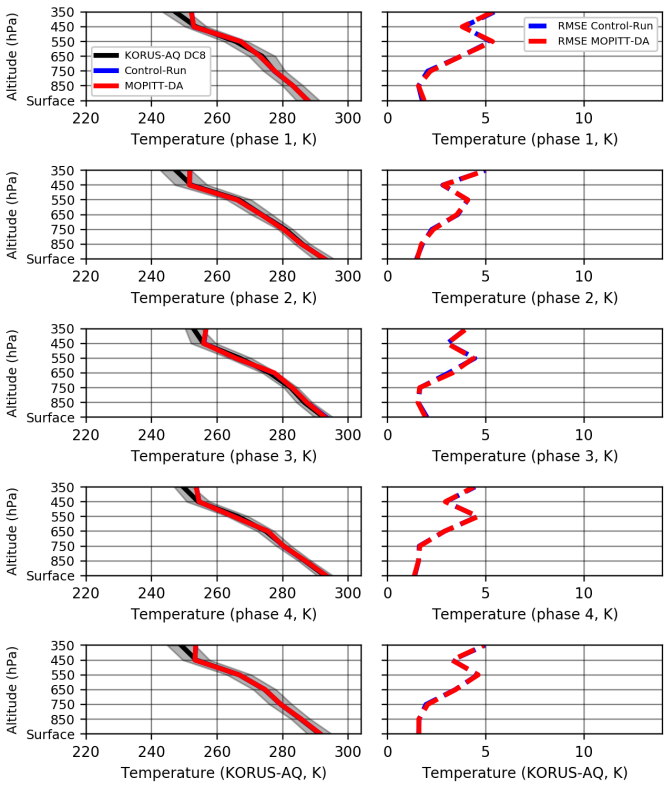

Figure S4: Average temperature profiles (left panels) and related RMSE (right panels) for the Control-Run and the MOPITT-DA. The mean (black line) and standard deviation (shaded grey) of the observations are calculated for each 100 hPa bins. The first 4 rows are average over the different weather regimes of the campaign (Peterson et al. 2019). The last row is the average over the whole campaign. The only rejected observations are when Benzene measured by the Proton Transfer Reaction – Mass Spectrometry (PTRMS) is higher than 1 ppb, measured only over the highly industrialized Daesan petrochemical complex (Simpson et al., 2020).

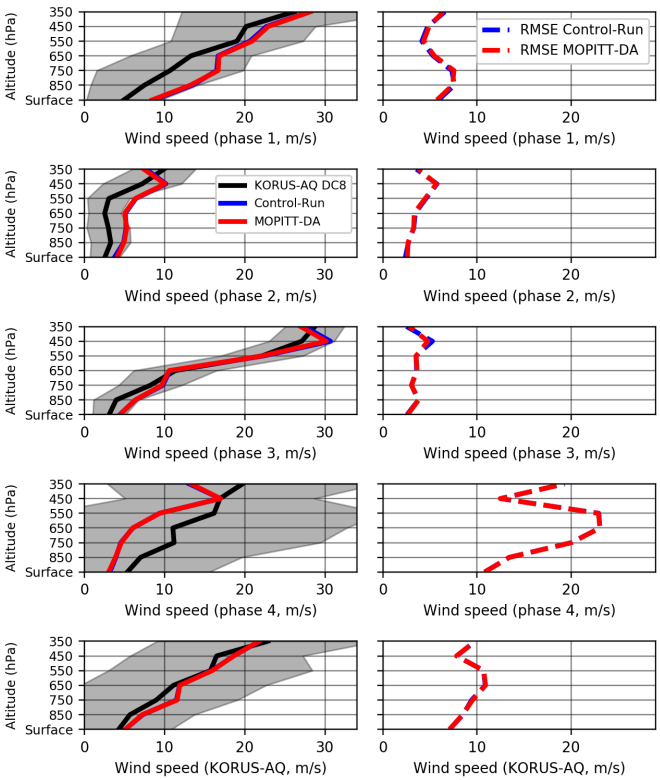

Figure S5: Average wind speed profiles (left panels) and related RMSE (right panels) for the Control-Run and the MOPITT-DA. The mean (black line) and standard deviation (shaded grey) of the observations are calculated for each 100 hPa bins. The first 4 rows are average over the different weather regimes of the campaign (Peterson et al. 2019). The last row is the average over the whole campaign. The only rejected observations are when Benzene measured by the Proton Transfer Reaction – Mass Spectrometry (PTRMS) is higher than 1 ppb, measured only over the highly industrialized Daesan petrochemical complex (Simpson et al., 2020).

3.Nudging experiments

When no data assimilation is performed, the dynamic from the prognostic variables U, V, and T needs to be nudge to a reanalysis data set to reproduced the meteorological variability. The nudging is driven by the strength, a normalized coefficient that ranges between 0 and 1 and the frequency of the nudging, here set-up to use every 6 hourly outputs from either the GEOS5 reanalysis or our own CAM-Chem/DART Control-Run. We performed an ensemble of simulations that can be either nudged to GEOS5 or DART, uses the prior or the posterior emissions, and with different values shown in Table S1. We first discarded the simulations with lower nudging coefficients, i.e. with a weaker reanalysis weight, that were not able to catch the weather variability and were showing larger errors against the DC8 measurements. We also found that having a weight that is too strong can lead to unrealistic values, unrealistic temperature fields were modelled when using the U, V and T set to 0.72 with a nudging to GEOS5.
The sensitivity simulations were then based on the g-prior-0.72, which show the lower RMSE for water vapor, temperature and wind speed.

Simulation name	nudging	U, V, T (nudge)
g-prior-0.24	GEOS5	0.24, 0.24, 0.24
d-prior-0.24	DART	0.24, 0.24, 0.24
g-prior-0.48	GEOS5	0.48, 0.48, 0.48
d-prior-0.48	DART	0.48, 0.48, 0.48
g-prior-0.72	GEOS5	0.72, 0.72, 0.48
d-prior-0.72	DART	0.72, 0.72, 0.72

Table S1: List of the nudging simulations experiments, the 6 hourly outputs from the reanalysis data (GEOS5) or from the Control-Run are used but linear physic tendencies are applied at the model physic time step (30 Min).

Wind Speed	simulations	RMSE	r	Bias
	prior-d-0.24	9.21	0.61	1.32
	prior-d-0.48	8.96	0.63	1.22
	prior-d-0.72	8.87	0.63	1.11
	prior-m-0.24	8.89	0.64	1.32
	prior-m-0.48	8.61	0.65	1.01
	prior-m-0.72	8.56	0.66	0.92
H2O	**simulations**	**RMSE**	**r**	**Bias**
	prior-d-0.24	2990.14	0.86	766.62
	prior-d-0.48	2570.17	0.89	498.83
	prior-d-0.72	2459.9	0.89	396.89
	prior-m-0.24	2429.31	0.89	32.67
	prior-m-0.48	2191.41	0.91	-68.4
	prior-m-0.72	2126.97	0.91	-98.73
Temperature	**simulations**	**RMSE**	**r**	**Bias**
	prior-d-0.24	2.95	0.98	1.09
	prior-d-0.48	2.88	0.98	1.03
	prior-d-0.72	2.85	0.99	1.01
	prior-m-0.24	2.88	0.98	0.96
	prior-m-0.48	2.81	0.99	0.93
	prior-m-0.72	2.79	0.99	0.94

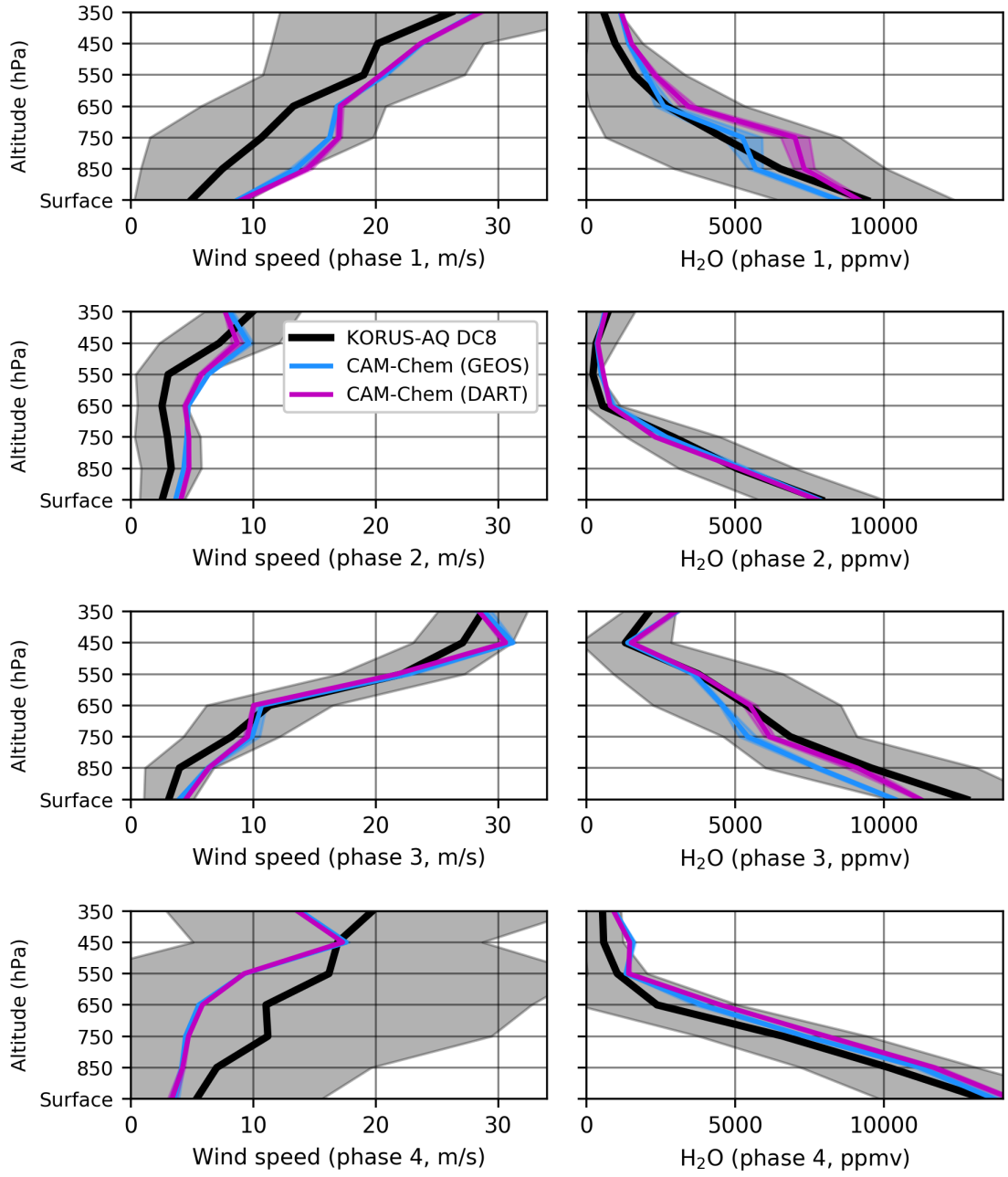

Figure S6: ***Average wind speed profiles (left panels) and water vapor (right panels) for the set of DART and the set of GEOS nudging experiments. The mean (black line) and standard deviation (shaded grey) of the observations are calculated for each 100 hPa bins. The 4 rows correspond to averages over the different weather regimes of the campaign.***

4.Sensitivity to biogenic emissions

To further evaluate the sensitivity to the biogenic emissions, emissions are increased based on the Plant Functional Types (PFTs) found in Korea, the "Needleleaf Evergreen Temperate Tree", "Broadleaf Evergreen Temperate Tree", "Broadleaf Deciduous Temperate Tree". All the other PFTs are held the same. Profiles of observed VOCs that have primarily a biogenic source such as Methanol (CH_3OH), Ethene (C_2H_4), Acetaldehyde (CH_3CHO), Acetone (CH_3COCH_3) are used for evaluation. The Methyl hydroperoxide (CH_3OOH) and Formaldehyde (CH_2O) are mostly formed in the atmosphere, but mostly from the oxidation of biogenic compounds closer to the source. The tables S2 show the different sensitivity experiments that were motivated by the vertical profile comparison.

	CH3OH	CH3CHO	CH2O	C2H4	Others
g-post-0.72	1	1	1	1	1
g-post-0.72-MEGAN-1	2	2	2	2	2
g-post-0.72-MEGAN-2	4	4	1	/2	2
g-post-0.72-MEGAN-3	4	4	1	/2	1.66

Table S2: Increase factor compare to the base MEGAN 2.1 for the 3 different simulations, the same factor is only applied to the following PFTs "Needleleaf Evergreen Temperate Tree", "Broadleaf Evergreen Temperate Tree", "Broadleaf Deciduous Temperate Tree".

Figure S7 show the comparison of the different simulations with observations and Fig. S8 show the map of the emissions of isoprene. The emissions for the C_2H_4 were decreased since the concentrations were overestimated. This could be due to an overestimation to its minor anthropogenic source. In the g-post-0.72-MEGAN-2 and g-post-0.72-MEGAN-3, we increase CH_3OH and CH_3CHO by a factor of 4 instead of 2, since the bias was particularly large and a lower scaling factor was applied to the other VOCs for the g-post-0.72-MEGAN-3. Aside from those VOCs, the metric was the surface (the first layer) CH_2O concentrations. The objective is to see how much this impacts the CO. Overall, the increase in CO was mostly at the surface, with an increase of 5 ppbv, which is a rather limited impact.

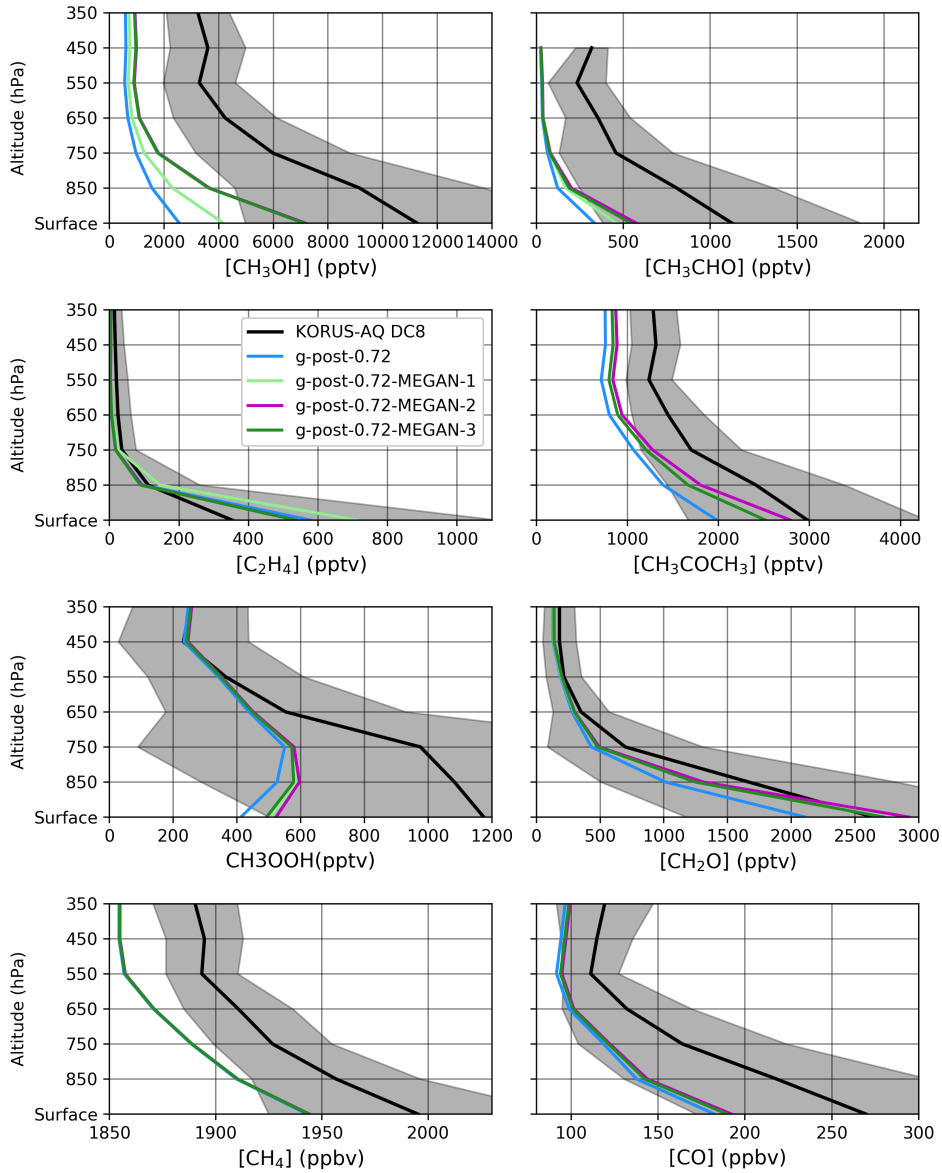

Figure S7: Average vertical profiles for Methanol (CH3OH), Ethene (C2H4), Acetaldehyde (CH3CHO), Acetone (CH3COCH3), Methyl hydroperoxide (CH3OOH), Formaldehyde (CH2O), Methane (CH4) and CO. The data are filtered if the Benzene measured by the PTRMS is higher 1 ppbv, otherwise the average is for all the DC8 flights.

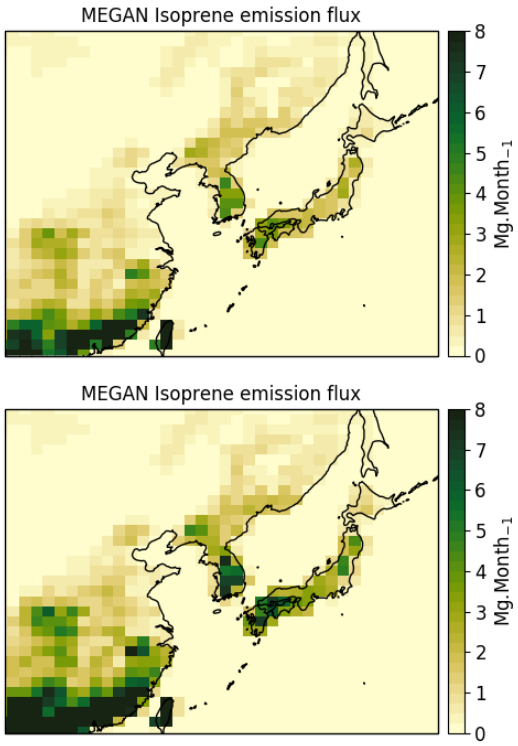

Figure S8: MEGAN isoprene emissions flux for May 2016 for the reference simulation (top panel, g-post-0.72) and for the second alternative simulation (bottom panel g-post-0.72-MEGAN-2).

References

Gaubert, B., Arellano, A.F., Barré, J., Worden, H.M., Emmons, L.K., Tilmes, S., Buchholz, R.R., Vitt, F., Raeder, K., Collins, N., Anderson, J.L., Wiedinmyer, C., Martínez-Alonso, S., Edwards, D. P., Andreae, M. O., Hannigan, J. W., Petri, C., Strong, K., and Jones, N.: Toward a chemical reanalysis in a coupled chemistry-climate model: An evaluation of MOPITT CO assimilation and its impact on tropospheric composition. Journal of Geophysical Research: Atmospheres, 121(12), pp.7310-7343, https://doi.org/10.1002/2016JD024863, 2016.

Peterson, D.A., Hyer, E.J., Han, S.-O., Crawford, J.H., Park, R.J., Holz, R., Kuehn, R.E., Eloranta, E., Knote, C., Jordan, C.E. and Lefer, B.L.: Meteorology influencing springtime air quality, pollution transport, and visibility in Korea. Elem Sci Anth, 7(1), p.57. DOI: http://doi.org/10.1525/elementa.395, 2019.